Research Article Vol. 28, No. 16 / 3 August 2020 / Optics Express 23739
Optics EXPRESS

# Resonant-cavity-enhanced responsivity in germanium-on-insulator photodetectors

SOUMAVA GHOSH,[1,2,3] KUAN-CHIH LIN,[2] CHENG-HSUN TSAI,[2] KWANG HONG LEE,[4] QIMIAO CHEN,[5] BONGKWON SON,[5] BRATATI MUKHOPADHYAY,[3] CHUAN SENG TAN,[4,5] AND GUO-EN CHANG[1,2,*]

[1] *Department of Mechanical Engineering, and Advanced Institute of Manufacturing with High-Tech Innovations (AIM-HI), National Chung Cheng University, Chiayi 62102, Taiwan*
[2] *Graduate Institute of Opto-Mechatronics, National Chung Cheng University, Chiayi 62102, Taiwan*
[3] *Institute of Radio Physics and Electronics, University of Calcutta, Kolkata 700009, India*
[4] *Low Energy Electronic Systems (LEES), Singapore MIT Alliance for Research and Technology (SMART), Singapore*
[5] *School of Electrical and Electronic Engineering, Nanyang Technological University, Singapore*
[*] *imegec@ccu.edu.tw*

**Abstract:** The germanium-on-insulator (GOI) has recently emerged as a new platform for complementary metal-oxide-semiconductor (CMOS)-compatible photonic integrated circuits. Here we report on resonant-cavity-enhanced optical responses in Ge photodetectors on a GOI platform where conventional photodetection is difficult. A 0.16% tensile strain is introduced to the high-quality Ge active layer to extend the photodetection range to cover the entire range of telecommunication C- and L-bands (1530–1620 nm). A carefully designed vertical cavity is created utilizing the insulator layer and the deposited $SiO_2$ layer to enhance the optical confinement and thus optical response near the direct-gap absorption edge. Experimental results show a responsivity peak at 1590 nm, confirming the resonant cavity effect. Theoretical analysis shows that the optical responsivity in the C- and L-bands is significantly enhanced. Thus, we have demonstrated a new type of Ge photodetector on a GOI platform for CMOS-compatible photonic integrated circuits for telecommunication applications.

© 2020 Optical Society of America under the terms of the OSA Open Access Publishing Agreement

## 1. Introduction

High speed and low noise make optical communication very attractive for long-distance communication applications. Photodetectors (PDs) are crucial for high-performance electro-optic conversion. While commercially available III–V compound semiconductors are inherently suitable for present fiber-optic telecommunication windows (1265–1675 nm) [1,2], research attention has recently shifted to group-IV PDs because of their complementary metal-oxide-semiconductor (CMOS) compatibility, which enables large-scale, compact, low-cost electronic-photonic integrated circuits (EPICs). Unfortunately, Si PDs cannot be used for fiber-optic optical communication because the cutoff wavelength of their absorption spectrum is ~1100 nm [3]. On the other hand, Ge, another CMOS-compatible group-IV semiconductor, has a smaller direct bandgap (0.8 eV) than Si, corresponding to a direct-gap absorption cutoff wavelength of 1550 nm [4]. This makes Ge PDs very promising for EPICs used in long-distance telecommunication applications.

Although Ge PDs show promising performance for telecommunication, there are practical challenges to overcome. First, the optical response of a Ge PD rolls off very rapidly beyond 1500 nm [4–6], making efficient photodetection difficult in the most important telecommunication C-band (1530–1565 nm) and L-band (1565–1620 nm), widely used by dense wavelength division multiplexing (DWDM) technology that significantly enhances the data transport rate. The direct

#398046 https://doi.org/10.1364/OE.398046
Journal © 2020 Received 19 May 2020; revised 17 Jul 2020; accepted 17 Jul 2020; published 27 Jul 2020

bandgap of Ge can be reduced by Sn-alloying [6–9] and by imparting tensile strain to extend the photodetection range [10–12]. By directly growing Ge on Si, a tensile strain of ~0.2% can be introduced, redshifting the direct-gap absorption edge and thus covering the telecommunication C-band and a large part of the L-band. However, epitaxy of Ge on Si leads to a defective Si/Ge interface due to the large lattice mismatch (>4%) between Si and Ge, degrading the material quality and thus device performance. In addition, the optical confinement between Si and Ge is weak, because their refractive indices differ only slightly. Although growing Ge on Si-on-insulator (SOI) substrates can enhance the optical confinement and thus the optical responsivity [13], the problem of the defective Ge/Si interface remains.

Recently, Ge-on-insulator (GOI) platforms have attracted increasing attention for future CMOS-compatible electronic and photonic applications. The quality of the Ge layer can be significantly improved compared to that of Ge-on-Si structures, as the defective region which increases the dark current of Ge PDs is absent [14–18]. In addition, the introduction of an insulator layer between the Si and Ge can provide better optical confinement for the Ge active layer, enhancing the optical responses of the devices. To date, only a few Ge PDs on GOI have been demonstrated with photodetection range extended by tensile strain [14–17]. However, very little has been done to enhance the optical responsivity of Ge PDs on GOI by improving the optical confinement of the Ge active layer.

In this letter, we demonstrate, to the best of our knowledge for the first time, resonant-cavity-enhanced responsivity in Ge PDs on a GOI platform for efficient photodetection in the telecommunication C- and L-bands. A tensile strain is introduced into the Ge layer to reduce the direct bandgap, thereby extending the photodetection range. In addition, the insulator in the GOI platform provides excellent optical confinement because it has a much smaller refractive index than Ge, and thereby creates a vertical cavity for enhancing the optical responsivity of the device. By carefully designing the vertical cavity, the optical responsivity of the Ge PD near the absorption band edge can be significantly enhanced, and thus efficient photodetection in the telecommunication C- and L-bands can be achieved.

## 2. Device design

Figure 1(a) illustrates the design of our surface-illuminated Ge PD on a GOI platform. The GOI sample used in this study was fabricated using wafer-bonding and layer transfer techniques [16]. The layer structure, consisting of a top Ge layer and an insulator layer comprising 312-nm-thick $SiO_2$, 50-nm-thick SiN, and 216-nm-thick $SiO_2$ layers, is schematically displayed in Fig. 1(b). Note that although the top Ge layer was unintentionally doped, it has an *n*-type background doping concentration of $\sim 6 \times 10^{16}$ cm$^{-3}$. The top Ge layer acts as the photon-absorbing layer. It is passivated by a $SiO_2$ layer. Two metal pads are placed on top of the Ge layer. Carriers can be generated in the Ge active layer when it is illuminated by normally incident photons. When a bias voltage is applied across the metal pads, the induced electric field sweeps the photogenerated carriers to the metal pads, causing an electric current to flow. In addition, because of the large contrast between their refractive indices ($n \sim 1.45$) and that of Ge ($n \sim 4.2$), the insulator and the deposited $SiO_2$ layer act as the bottom and top reflectors of a vertical cavity capable of effective optical confinement, thus enabling a multiple-pass reflection scheme and recycling of light not initially absorbed by the Ge active layer. When the resonant condition is reached, the light field in the cavity can be built up by constructive interference, thereby enhancing the responsivity.

The resonant conditions are strongly dependent on the cavity length (the thickness of the Ge active layer, $t$). This length must be carefully designed to shift the resonant wavelength to the detection wavelength region of interest, in this case that of the telecommunication C- and L-bands. Finite-element-method (FEM) analysis was performed to determine the resonant wavelength of the device and the field distribution; a plane wave was used as the light source and the material dispersion was taken into account [19]. Figure 1(c) shows simulated reflectivity

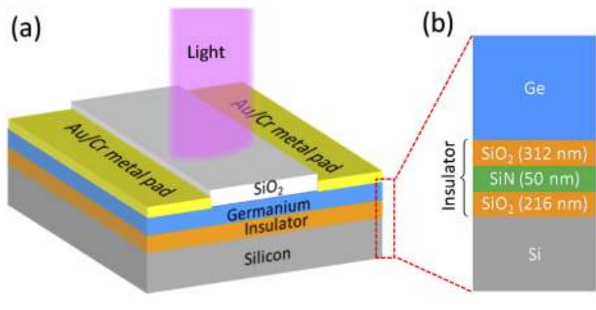


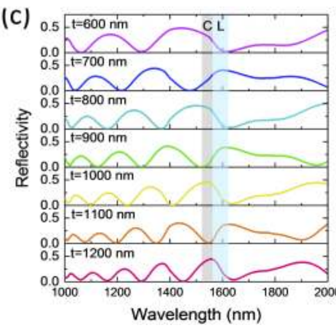


**Fig. 1.** (a) Schematic diagram of resonant-cavity-enhanced Ge photodetector on a Ge-on-insulator (GOI) platform. (b) Layer structure of the GOI platform. (c) Simulated reflectivity spectra at the air/$SiO_2$ interface of the device with different Ge thicknesses.

at the air/$SiO_2$ interface of the device with different Ge layer thicknesses. The spectra display ripple structures attributed to the interference in the layers; the reflectivity minima represent constructive interference in the cavity [20]. As the thickness of the Ge active layer increases, these reflectivity minima redshift. Since we aim to enhance the responsivity of the device in the C- and L-bands, the optimal thickness of the Ge layer is in the range of 900–1000 nm. Based on the simulation results, the thickness of the top Ge layer in the GOI sample was carefully thinned by chemical-mechanical planarization (CMP) to the target thickness, and a thickness of 960 nm was achieved.

## 3. Material characterization

The sample was characterized by cross-sectional transmission electron microscopy (XTEM), atomic force microscopy (AFM), and Raman microscopy; the results are presented in Fig. 2. Figure 2(a) shows the XTEM image of the sample, reveal clear and flat interfaces between layers. Figures 2(b) and 2(c) show the high-resolution XTEM images in the Ge layer and at the Ge/$SiO_2$ interface. No apparent threading dislocations were observed since the defective region has been removed. A flat surface with an excellent root mean square (RMS) roughness of only 0.4 nm was obtained. Figure 2(d) shows the AFM image of the surface of the GOI sample. In addition, from etch-pit experiments, we obtained an average threading dislocation density (TDD) of $2.5 \times 10^7 cm^{-2}$ for the GOI sample, which is comparable with good-quality Ge films on silicon substrates with a typical TDD of $2 \times 10^7 cm^{-2}$ [18]. These results confirm the good material quality of the GOI sample. Figure 2(e) shows the measured spectrum compared with that of bulk Ge. (The Raman experiments were carried out using a 532 nm laser under a back-scattering scheme in which the LO-mode phonon was measured. The light penetration depth ($d$) for the 532 nm laser was estimated to be ~20 nm from $d$=1/α, where α is the absorption coefficient and the value for Ge at 532 nm is 577214 $cm^{-1}$ [19], ensuring the detection of Raman signals from the Ge layer only.) For bulk Ge, a peak at 300 $cm^{-1}$ was observed, associated with the Ge-Ge LO phonon mode. For the GOI sample, the Ge-Ge LO phonon mode was observed at 299.31 $cm^{-1}$. This shift is attributable to the strain induced during the fabrication of the sample, indicating that the top Ge layer was biaxially stressed. The in-plane strain level ($\varepsilon$) can be deduced from the Raman shift ($\Delta\omega$) by the equation $\Delta\omega = b \times \varepsilon$. Using $b = -415$ $cm^{-1}$ [21], $\varepsilon = 0.16\%$ is obtained. This tensile strain is attributed to the difference between thermal expansion coefficient of Si and Ge during the Ge-on-Si growth [10], and it can slightly reduce the direct bandgap from 0.8 eV to 0.77 eV, according to calculations using deformation potential theory [22,23]. The direct-gap absorption edge is thereby extended from 1550 nm to 1610 nm.

Optics EXPRESS

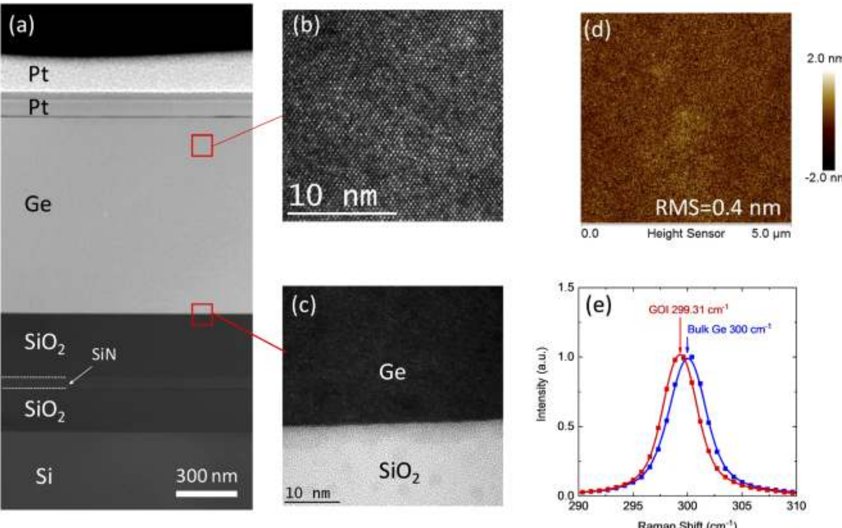


**Fig. 2.** Material characterization results of the Ge-on-insulator (GOI) sample. (a) Cross-sectional transmission electron microscopy (XTEM) image. High-resolution XTEM images in (b) the Ge layer and (c) at the Ge/$SiO_2$ interface. (d) Atomic force microscopy image, showing a low surface roughness. (d) Raman spectrum compared with that of bulk Ge.

## 4. Characterization of GOI photodetectors

The sample was fabricated into PDs using CMOS-compatible processing. A square mesa with a width of 1000 μm was defined using optical lithography with reactive ion etching (RIE) techniques. A 180-nm-thick $SiO_2$ passivation layer was then deposited using an e-beam evaporator. Contact windows were created using wet-etching techniques with a buffered oxide etch (BOE) etcher that provided excellent etching selectivity between $SiO_2$ and Ge. Finally, rectangular Au/Cr metal pads with a thickness of 200/20 nm were deposited and patterned using an e-beam evaporation together with lift-off techniques. A top-view scanning electron microscope (SEM) image of the fabricated device is shown in the inset of Fig. 3. Figure 3 shows the room-temperature current-voltage (*I-V*) characteristics of a fabricated GOI PD measured using a Keithley 2400 sourcemeter, both in a dark environment and when illuminated by a 1550-nm laser beam having an optical power of 0.77 mW. For the dark current, a linear *I-V* relationship was found, revealing good Ohmic contact between the metal and the semiconductor without any thermal annealing steps. In addition, symmetrical *I-V* characteristics were obtained under forward- and reverse-bias because of the symmetrical electrode design. From the slope of the *I-V* curve, the dark resistance was found to be 31.87 kΩ. When the PD was illuminated, the *I-V* curve remained linear, and the current significantly increased because of the photo-generated carriers. These results provide clear evidence for photodetection.

Figures 4(a) and 4(b) shows the room-temperature reflectivity at the top surface and optical responsivity spectra of the GOI PD with different applied bias voltages, measured using Fourier transform infrared spectroscopy and calibrated using a commercial extended InGaAs PD (Thorlabs DET10D2). The reflectivity spectrum exhibits oscillation features with minima located at 1380 nm and 1625 nm with a free spectrum range of ~245 nm, confirming the optical cavity effect. In contrast to the smooth responsivity spectra of conventional Ge PD without a cavity [10,16], the responsivity spectra of our device show two peaks at 1370 nm and 1561 nm. The former matches the position of the reflectivity minimum at 1380 nm very well. For the responsivity peak at 1561 nm, the position does not match the reflectivity minimum at 1625 nm. This observation

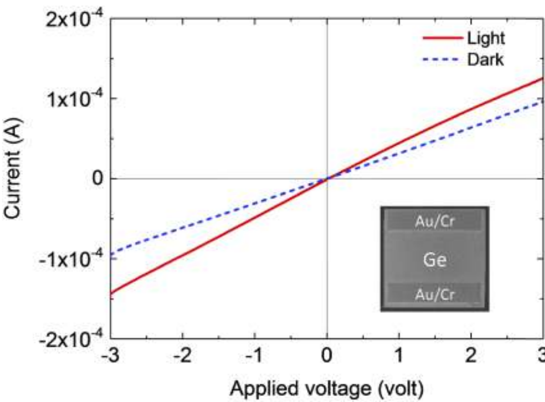


**Fig. 3.** Current-voltage characteristics of the Ge-on-insulator resonant-cavity-enhanced photodetector in a dark environment (blue dashed line) and with 1550 nm, 0.77 mW illumination (red solid line). The inset shows a scanning electron microscope (SEM) image of the fabricated device.

is attributed to that fact that the resonant wavelength lies on the falling edge of the absorption coefficient spectrum, as shown in Fig. 4(c). As the responsivity is a function of reflectivity and absorption coefficient, the responsivity peak occurs at a smaller wavelength than the reflectivity peak. At resonant condition, the reduced reflectivity suggests that more photons enter the device and are absorbed by the Ge active layer then transferred to photocurrents. As the applied bias

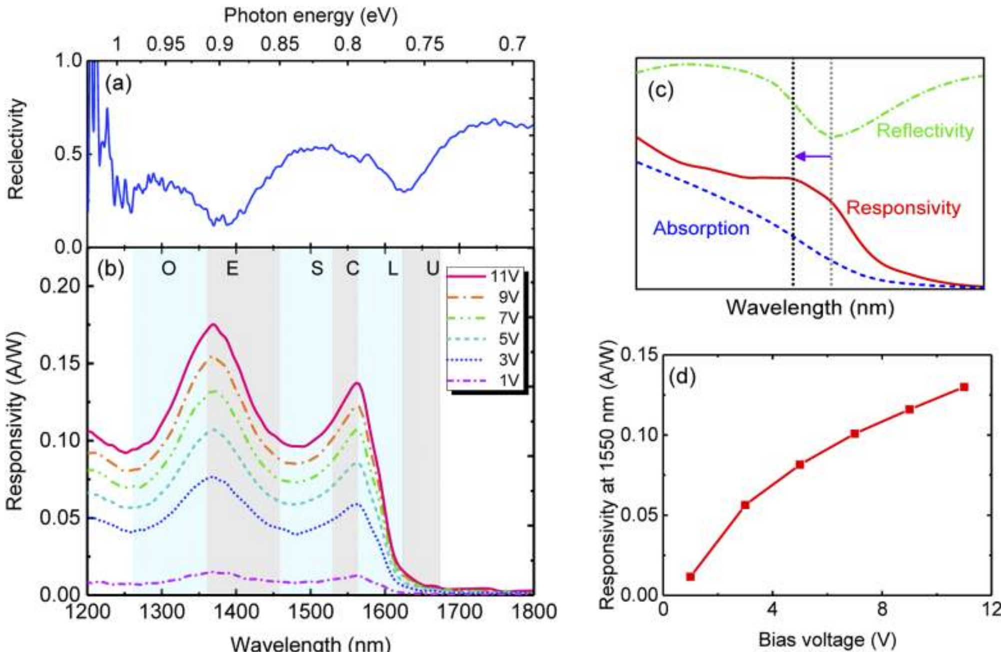


**Fig. 4.** Measured (a) reflectivity and (b) responsivity spectra of the GOI PD with different applied bias voltages at room temperature. (c) Schematic plot of reflectivity, absorption coefficient, and responsivity spectra near the direct-gap absorption edge. (d) Measured responsivity at 1550 nm as a function of applied bias voltage.

voltage rises, the responsivity significantly increases. Figure 4(d) shows the responsivity at 1550 nm as a function of the applied bias voltage, showing that the responsivity increases with increasing bias voltage, but tends to saturate when the applied voltage is high. This observation is attributed to the stronger electric field in the device that enhances the carrier collection efficiency. In particular, a resonant peak is found at 1561 nm, indicating that responsivity in the telecommunication C-band is significantly enhanced. As the wavelength increases further, the responsivity decreases, and becomes small at 1621 nm. These results suggest that the photodetection range of our device entirely covers the telecommunication O-, E-, S-, C-, and L-bands. Beyond 1621 nm, the responsivity becomes small, since only inefficient indirect interband transitions provide optical absorption. These results demonstrate the effectiveness of combining tensile strain with a resonance cavity in a high-quality GOI platform for enhancing the optical responsivity of a Ge PD. We anticipate that the resonant wavelength of the cavity can also be widely varied by engineering the cavity length (the thickness of the Ge active layer, as shown in Fig. 1(c)) to amplify the optical responsivity at other wavelengths of interest. It is noted that the responsivity values are not higher than the reported values in Ge PDs [5,10,11], which can be attributed to the device structure and the thickness of the Ge active layer. We believe that further optimization of the device structures could also enhance the device performance.

## 5. Numerical simulations and discussion

To gain a deeper understanding of the resonant-cavity-enhanced responsivity in the Ge PD on GOI, theoretical analysis was performed on the responsivity. We start with the calculation of the strained bandgap energies and absorption coefficient. The strained bandgap energies were calculated using deformation potential theory [22,23], and the strained band structures were calculated using a multi-band **k·p** method taking into account the band nonparabolicity effect [23,24]. The direct-gap absorption coefficient was then calculated using Fermi's golden rule with a Lorentzian lineshape [23–25]:

$$\alpha(\hbar\omega) = \frac{\pi\hbar e^2}{n_r c\varepsilon_0 m_0^2 \hbar\omega}\sum_m \int \frac{2d\mathbf{k}}{(2\pi)^3}|\hat{e}\cdot p_{CV}|^2 \times \frac{\gamma/(2\pi)}{[E_{C\Gamma}(\mathbf{k}) - E_m(\mathbf{k}) - \hbar\omega]^2 + (\gamma/2)^2} \tag{1}$$

where $n_r$ is the refractive index, $c$ is the speed of light in free space, $e$ is the electronic charge, $\hbar$ is the reduced Planck's constant, $m_0$ is the free electron mass, $\varepsilon_0$ is the free-space permittivity, $\omega$ is the angular frequency of incident light, $|\hat{e}\cdot p_{CV}|^2 = m_0E_p/6$ is the momentum matrix with $E_p$ being the photon energy, $\gamma$ is the full-width-at-half-maximum (FWHM) of the Lorentzian lineshape ($\gamma = 15$ meV is used), and $E_{C\Gamma}(\mathbf{k})$ and $E_m(\mathbf{k})$ are the electron and hole energies in the direct conduction band and valence band, respectively, with $m$ indicating the heavy-hole (HH) and light-hole (LH) bands. Here interband transitions from the HH band to the Γ-conduction band (HH→cΓ) and from the LH band to the Γ-conduction band (LH→cΓ) are considered. Here the absorption coefficient due to indirect-gap interband transitions is neglected because it is much smaller than the direct-gap absorption.

Figure 5(a) shows the schematic band structure for 0.16% tensile-strained Ge at $T$=300K. For bulk Ge, the direct bandgap is 0.8 eV. When a 0.16% tensile strain is present, the direct conduction band and valence band edges are shifted, and the LH band is pushed above the HH band, so the LH→cΓ transition energy defines the direct-gap absorption edge. The calculated HH→cΓ transition and LH→cΓ transition energies are 787 meV and 770 meV, respectively. Figure 5(b) shows the calculated direct-gap absorption spectra for bulk Ge and 0.16% tensile-strained Ge at $T$=300K. The direct-gap absorption edge, defined by the LH→cΓ transition energy, is shifted to 1610 nm, which is in good agreement with the experimental results. With the shift of direct-gap absorption edge, the optical absorption coefficient for 0.16% tensile-strained Ge is enhanced compared to that of bulk Ge, which can improve the optical responsivity.

Optics EXPRESS

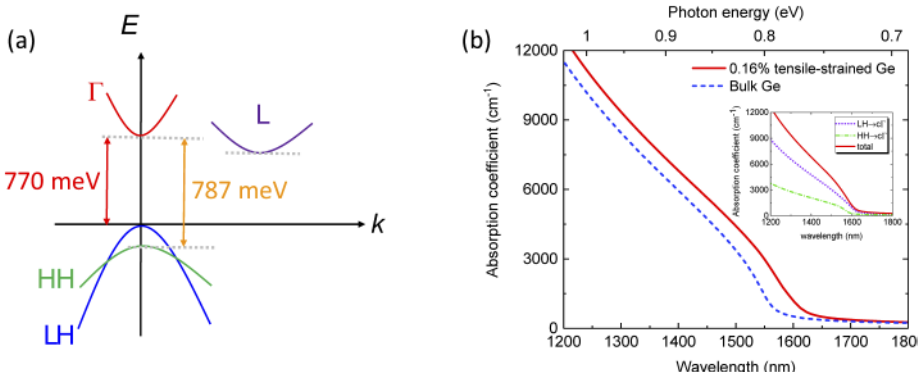


**Fig. 5.** (a) Schematic band structure for 0.16% tensile-strained Ge. (b) Calculated absorption spectra for bulk Ge and 0.16% tensile-strained Ge at $T = 300$ K. The inset shows the optical absorption spectra for HH→cΓ and LH→cΓ interband transitions and their superposition for 0.16% tensile-strain Ge.

After the absorption coefficient was calculated, we investigated the resonant-cavity-enhanced responsivity of the GOI PD. Here we theoretically compare the responsivity of the GOI PD (with cavity) with that of the Ge-on-Si PD (without cavity) with a 960-nm-thick, 0.16% tensile-strained Ge active layer to show the enhancement in responsivity. FEM simulations were performed using a plane wave as the light source. In the simulation, the absorption coefficient of the Ge active layer is taken from Fig. 5(b) and the wavelength-dependent refractive indices of the materials are taken from Ref. [19]. The field distributions in the structures and the reflectivity, transmissivity, and optical absorption of the Ge active layer were then calculated. Assuming an internal quantum efficiency of unity, we then calculated the optical responsivity from the optical absorption within the Ge active layer. Figures 6(a) and 6(b) shows the calculated reflectivity at the air/$SiO_2$ interface and responsivity spectra for Ge-on-Si and GOI PD structures, respectively. For the Ge-on-Si structure, the reflectivity spectrum exhibits slight oscillation features due to the interference in the layers. The responsivity decreases with increasing wavelength, and becomes very small near 1610 nm, corresponding to the direct-gap absorption edge of the 0.16% tensile-strained Ge active layer. On the other hand, for the GOI PD, the reflectivity spectrum shows stronger oscillation structures than that of the Ge-on-Si structure in which the reflectivity minima represent the resonant conditions. Two reflectivity minima were found at 1370 nm and 1590 nm, which are in good agreement with the experimental results as shown in Fig. 3(a). The discrepancy may arise from the refractive indices of the materials used in the simulations. In addition, the reflectivity of the GOI PD at resonant conditions is smaller than that of the Ge-on-Si structure, indicating that less light is reflected by the structure and more light can enter the GOI PD. As a result, the responsivity of the GOI PD is significantly larger than that of the Ge-on-Si PD at resonant conditions, as shown in Fig. 6(b). The inset in Fig. 6(b) shows the calculated enhancement factor for responsivity in the telecommunication C- and L bands, which is defined as the ratio of the responsivity of the GOI PD to that of the Ge-on-Si PD. The responsivity can be enhanced up to a factor of 171% for the GOI PD in the spectral range, showing the effectiveness of using a resonant cavity to enhance the responsivity. To further confirm the resonant-cavity effect, Figs. 6(c) and 6(d) shows the simulated optical field for GOI and Ge-on-Si PD structures, respectively, at resonant conditions (1590 nm). For the Ge-on-Si PD structure, as shown in Fig. 6(c), despite strong reflection of the incident light at the air/$SiO_2$ interface, a certain amount of light can enter the structures. However, the small contrast in refractive index between Ge ($n$~4.2) and Si ($n$~3.45) cannot provide effective optical confinement for the light, resulting in weak light intensity in the Ge active layer. On the other hand, for the GOI PD structure, as shown in Fig. 6(d), a significant

amount of light can enter the Ge active layer due to the lower reflectivity at resonant conditions. In addition, the light propagating in the Ge active layer can experience strong reflection at the air/$SiO_2$ and insulator/Si interfaces because of the high refractive contrast between Ge ($n$~4.2) and $SiO_2$ ($n$~1.45), developing a clear standing wave pattern to enhance the light intensity in the Ge active layer. The squared electric field in the Ge active layer for the GOI structure is significantly larger than that for the Ge-on-Si structure by a factor of 187% at resonant conditions (1590 nm), confirming better optical confinement in the GOI structure. These results suggest that the resonant-cavity effect significantly enhances the optical responsivity to enable sensitive photodetection in the telecommunication C- and L-bands. Given their extended photodetection range, enhanced optical responsivity, and CMOS-compatibility, we conclude that Ge PDs on GOI platforms are promising candidates for efficient optical receivers for telecommunication applications.

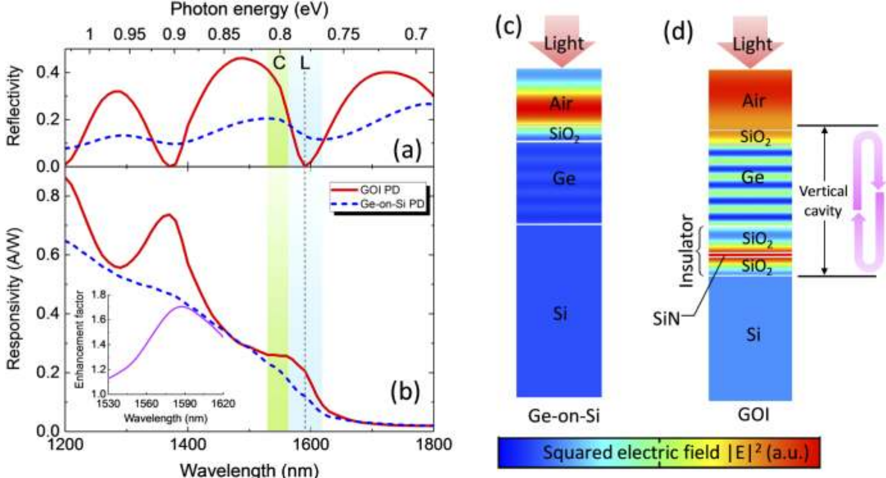


**Fig. 6.** (a) Calculated reflectivity and (b) calculated responsivity spectra for Ge-on-insulator (GOI) and Ge-on-Si photodetectors (PDs) at $T = 300$ K. The inset shows the responsivity enhancement factor for the GOI PD. Simulated optical field distribution of the (c) Ge-on-Si and (d) GOI PD structures at 1590 nm. The thickness of the Ge layer is fixed to 960 nm.

## 6. Conclusion

In conclusion, we have successfully demonstrated resonant-cavity-enhanced Ge photoconductors on a GOI platform. The high-quality top Ge layer is the active layer. Tensile strain can extend the photodetection range, and the resonant cavity created utilizing the insulator layer and the deposited $SiO_2$ layer significantly enhances the optical responsivity, enabling effective photodetection in the entire telecommunication C-band and L-band. This letter presents a new Ge photodetector integrable with Ge-based electronic-photonic integrated circuits for telecommunication applications.

## Funding

Ministry of Science and Technology, Taiwan (MOST 108-2221-E-194-055, MOST 109-2636-E-194-002); Ministry of Education of Taiwan; National Research Foundation Singapore Competitive Research Programme (NRF–CRP19–2017–01).

Optics EXPRESS

## Acknowledgments

The authors thank Miss Yue-Tong Jheng at CCU for providing assistance in the experiments.

## Disclosures

The authors declare no conflicts of interest.

## References

1. R. W. M. Hoogeveen, R. J. van der A, and A. P. H. Goede, "Extended wavelength InGaAs infrared (1.0-2.4 μm) detector arrays on SCIAMACHY for space-based spectrometry of the Earth atmosphere," Infrared Phys. Technol. **42**(1), 1–16 (2001).
2. Y. Arslan, F. Oguz, and C. Besikci, "Extended wavelength SWIR InGaAs focal plane array: Characteristics and limitations," Infrared Phys. Technol. **70**, 134–137 (2015).
3. M. J. Deen and P. K. Basu, "*Silicon Photonics: Fundamentals and Devices*," (Wiley, Chichester, 2012).
4. M. Jutzi, M. Berroth, G. Wohl, M. Oehme, and E. Kasper, "Ge-on-Si vertical incidence photodiodes with 39-GHz bandwidth," IEEE Photonics Technol. Lett. **17**(7), 1510–1512 (2005).
5. A. K. Okyay, A. M. Nayfeh, K. C. Saraswat, T. Yonehara, A. Marshall, and P. C. McIntyre, "High-efficiency metal-semiconductor-metal photodetectors on heteroepitaxially grown Ge on Si," Opt. Lett. **31**(17), 2565–2567 (2006).
6. H. H. Tseng, H. Li, V. Mashanov, Y. J. Yang, H. H. Cheng, G. E. Chang, R. A. Soref, and G. Sun, "GeSn-based p-i-n photodiodes with strained active layer on a Si wafer," Appl. Phys. Lett. **103**(23), 231907 (2013).
7. Y. H. Peng, H. H. Cheng, V. I. Mashanov, and G. E. Chang, "GeSn p-i-n waveguide photodetectors on silicon substrates," Appl. Phys. Lett. **105**(23), 231109 (2014).
8. Y. H. Huang, G. E. Chang, H. Li, and H. H. Cheng, "Sn-based waveguide p-i-n photodetector with strained GeSn/Ge multiple-quantum-well active layer," Opt. Lett. **42**(9), 1652–1655 (2017).
9. B. J. Huang, J. H. Lin, H. H. Cheng, and G. E. Chang, "GeSn resonant- cavity-enhanced photodetectors on silicon-on-insulator platforms," Opt. Lett. **43**(6), 1215–1218 (2018).
10. J. Liu, D. D. Cannon, K. Wada, Y. Ishikawa, S. Jongthammanurak, D. T. Danielson, J. Michel, and L. C. Kimerling, "Tensile strained Ge p-i-n photodetectors on Si platform for C and L band telecommunications," Appl. Phys. Lett. **87**(1), 011110 (2005).
11. H.-Y. Yu, D. Kim, S. Ren, M. Kobayashi, D. A. B. Miller, Y. Nishi, and K. C. Saraswat, "Effect of uniaxial strain on Ge p-i-n photodiodes integrated on Si," Appl. Phys. Lett. **95**(16), 161106 (2009).
12. G. E. Chang, S. W. Chen, and H. H. Cheng, "Tensile-strained Ge/SiGe quantum-well photodetectors on silicon substrates with extended infrared response," Opt. Express **24**(16), 17562–17571 (2016).
13. S. J. Koester, J. D. Schaub, G. Dehlinger, and J. O. Chu, "Germanium-on-SOI infrared detectors for integrated photonic applications," IEEE J. Sel. Top. Quantum Electron. **12**(6), 1489–1502 (2006).
14. J. R. Jain, D.-S. Ly-Gagnon, K. C. Balram, J. S. White, M. L. Brongersma, D. A. B. Miller, and R. T. Howe, "Tensile-strained germanium-on-insulator substrate fabrication for silicon-compatible optoelectronics," Opt. Mater. Express **1**(6), 1121 (2011).
15. J. H. Nam, F. Afshinmanesh, D. Nam, W. S. Jung, T. I. Kamins, M. L. Brongersma, and K. C. Saraswat, "Monolithic integration of germanium-on-insulator p-i-n photodetector on silicon," Opt. Express **23**(12), 15816 (2015).
16. Y. Lin, K. H. Lee, S. Bao, X. Guo, H. Wang, J. Michel, and C. S. Tan, "High-efficiency normal-incidence vertical p-i-n photodetectors on a germanium-on-insulator platform," Photonics Res. **5**(6), 702–709 (2017).
17. J. Kang, S. Takagi, and M. Takenaka, "Ge photodetector monolithically integrated with amorphous Si waveguide on wafer-bonded Ge-on-insulator substrate," Opt. Express **26**(23), 30546–30555 (2018).
18. K. H. Lee, S. Bao, G. Y. Chong, Y. H. Tan, E. A. Fitzgerald, and C. S. Tan, "Defects reduction of Ge epitaxial film in a germanium-on-insulator wafer by annealing in oxygen ambient," APL Mater. **3**(1), 016102 (2015).
19. E. D. Palik, *Handbook of Optical Constants of Solids* (Academic, 1985).
20. B. J. Huang, C. Y. Chang, Y. D. Hsieh, R. A. Soref, G. Sun, H. H. Cheng, and G. E. Chang, "Electrically injected GeSn vertical-cavity surface emitters on silicon-on-insulator platforms," ACS Photonics **6**(8), 1931–1938 (2019).
21. Y.-Y. Fang, J. Tolle, R. Roucka, A. V. G. Chizmeshya, J. Kouvetakis, V. R. D'Costa, and J. Menéndez, "Perfectly tetragonal, tensile-strained Ge on $Ge_{1-y}Sn_y$ buffered Si(100)," Appl. Phys. Lett. **90**(6), 061915 (2007).
22. G. E. Chang and H. H. Cheng, "Optical gain of germanium infrared lasers on different crystal orientations," J. Phys. D: Appl. Phys. **46**(6), 065103 (2013).
23. S. L. Chuang, *Physics of Photonic Devices*. (Wiley, New York, 2009), 2nd Ed.
24. G. E. Chang, R. Basu, B. Mukhopadhyay, and P. K. Basu, "Design and modeling of GeSn-based heterojunction phototransistors for communication applications," IEEE J. Sel. Top. Quantum Electron. **22**(6), 425–433 (2016).
25. S. Ghosh, B. Mukhopadhyay, and G. Chang, "Design and Analysis of GeSn-based Resonant-Cavity-Enhanced Photodetectors for Optical Communication Applications," IEEE Sensors J. **20**(14), 7801–7809 (2020).